Alma Mater Studiorum Università di Bologna
Archivio istituzionale della ricerca

Exploiting In-Hand Knowledge in Hybrid Joint-Cartesian Mapping for Anthropomorphic Robotic Hands

This is the final peer-reviewed author's accepted manuscript (postprint) of the following publication:

This version is available at: https://hdl.handle.net/11585/834307 since: 2021-10-05

Published:

DOI: http://doi.org/10.1109/LRA.2021.3078658

(Article begins on next page)

Exploiting In-Hand Knowledge in Hybrid Joint-Cartesian Mapping for Anthropomorphic Robotic Hands

Roberto Meattini, Davide Chiaravalli, Gianluca Palli and Claudio Melchiorri

Abstract—**Replication of human hand motions on anthropomorphic robotic hands is typically treated in literature as the combination of two sub-problems: the measurement of human hand motions, and the mapping of such motions on the robotic hand. In this work we focus on the second one. Different approaches have been proposed to deal with this problem, but none of them preserves both master finger shapes and fingertip positions on the robotic hand, i.e. ensuring predictability and natural motion for the teleoperator. In this article, we propose a novel hybrid approach that combines both joint and Cartesian mappings in a single solution. In particular, we exploit the a priori, in-hand information related to the areas of the workspace in which thumb and finger fingertips can get in contact. This allows to define, for each finger, a zone of transition from joint to Cartesian mapping. As a consequence, both hand shape during volar grasps and correctness of the fingertip positions for precision grasps are preserved, despite the master-slave kinematic dissimilarities. The proposed hybrid mapping is presented and experimentally evaluated both in simulation and with a real slave anthropomorphic robotic hand.**

Index Terms—**Multifingered Hands, Human-Centered Robotics, Human Factors and Human-in-the-Loop, Grasping, Dexterous Manipulation, Telerobotics and Teleoperation**

I. INTRODUCTION

Teleoperation of anthropomorphic robotic hands is still lacking of a general practical solution, notwithstanding the great technological advances in control and algorithms in the field of telerobotics during the last decades [1]. The emulation of teleoperator finger motions is anything but straightforward, due to the presence of kinematic dissimilarities between the master human hand and anthropomorphic robotic slave hand. For this reason, it is not possible to exactly reproduce the motion of each phalanx and, therefore, to obtain an intuitive and predictable behaviour of the slave hand [2].

In literature, related works can be classified in two human to robot hand mapping subproblems: *(i)* measurement, tracking and identification of human hand motions; *(ii)* mapping of human hand motions of the robotic hand. In the context of the present study, we will not focus on the first problem, which has been solved with good results by several sensor equipments,

such as sensorized gloves [3], marker-based/marker-less vision systems [4] or hand exoskeletons [5], along with advanced calibrations procedures [6]. We will therefore focus on the second problem, for the reason that it is a both conceptual and analytical problem which still lack of a general solution [7]. Among the many mapping methods proposed in literature, the most diffused are the direct joint [8] and direct Cartesian mappings [6]. Direct joint mapping is more appropriate for power grasps of big objects and gesture executions, since it consists in directly imposing the master hand joints on the slave hand, therefore preserving the finger shapes [9]. Direct Cartesian mapping consists in imposing the fingertip position and orientation on the slave hand, followed by the computation of the inverse kinematics to determine the input joint angles [10]. Generally, direct Cartesian mapping is suitable only for the execution of precision grasps, since it does not allow to preserve the master finger shapes [11], except in the case that an optimization problem is added with proper constraints. A specific more advanced mapping is the one based on the definition of a virtual object in the master hand workspace, which is then placed into the robotic hand workspace in order to obtain the coordinated fingertip positions [12]. Although this method can be extended to virtual objects of arbitrary shape [13], it can easily produce unintuitive slave hand motions when fingertips precision is required [14]. Other kinds of mapping approaches lie on the recognition of a set of master hand configurations corresponding to predefined robotic hand postures [15], [16]. These mappings are affected by the problem of generating unpredictable motions outside of the considered finite set of master hand configurations. A further interesting approach to teleoperation and mapping is provided by the Hidden Robot Concept [17], in which the slave robot is hidden to the operator by means of a virtual intermediate environment. As a matter of fact, methods proposed in literature mostly disregard the necessity of taking care about intuitiveness and predictability of the teleoperated motions. However, they should be conserved by preserving both Cartesian precision and finger shapes to some extent.

In this work, we propose a hybrid joint-Cartesian mapping exploiting an aspect poorly explored in previous works: the in-hand information available a priori. Specifically, we consider the areas of the master and slave hand workspaces in which the contact between thumb and finger fingertips is possible, and we exploit this constructional knowledge to realize a smooth transition between joint and Cartesian mappings. The exploitation of fingertips contact areas has been poorly investigated in previous hand mappings, although the importance of the thumb-finger workspace intersections is well known from specific studies [18], and we claim that it can be used
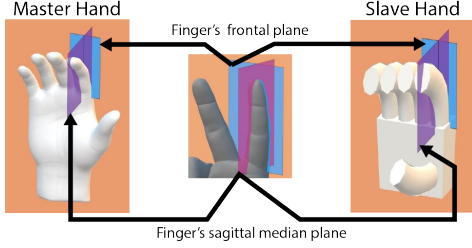
Fig. 1. Generic depiction of the master and slave hands, and related finger's sagittal median and frontal planes (illustrated only for the index finger.)

for improving the mapping of motions from the master hand to an anthropomorphic robotic hand. We therefore propose a hybrid master-to-slave hand mapping exploiting the thumb-fingers in-hand knowledge to enable a transition between joint and Cartesian mapping. This is guided by the rationale of preserving, within a single strategy, the master finger shapes during gesture and volar grasp executions (i.e. when thumb and finger fingertips are far away from each other), and correctness of the fingertip positioning during precision grasp/posture executions (i.e. when thumb and finger fingertips are typically very close.) In the following, the method is presented and then experimentally evaluated both in simulation and with a real anthropomorphic robotic hand.

II. METHODS

The proposed mapping is thought for robotic hands that are anthropomorphic. More specifically, note that the level of anthropomorphism of a robotic hand depends on multiple aspects related to kinematics, contact surfaces and hand size [19]. Therefore, it is appropriate to specify the minimum level of anthropomorphism required in the context of the present study. To match this requirement, referring to Fig. 1, the only assumptions we consider are that: *(i)* the master/slave hand models present a structure composed by a palm, an opposable thumb and fingers, and *(ii)* for each finger (hence different from the thumb) of the master/slave hand, it is possible to define a finger's sagittal median plane and frontal plane. That is, the same as it is possible to do with the human hand. Incidentally, with finger's sagittal median plane we refer to the plane equally dividing the right and left parts of the finger, and with the finger's frontal plane we mean the plane that equally divides the anterior and posterior parts of the finger (Fig. 1.)

A. Thumb-finger Convex Hull

In the following we will consider only the thumb and index finger, since the method is identically applied also for the others thumb-finger couples, and can therefore be immediately extended to the whole master/slave hand. Let us first of all consider the set of admissible joint configurations of the master hand's thumb, defined as

$$Q_T = \left\{ {}^M q_T \in \mathbb{R}^n : q_{\inf} \leq {}^M q_T \leq q_{\sup} \right\}, \qquad (1)$$

where the left superscript "M" indicates the master hand (also in the following), ${}^M q_T$ is the vector of n joint angles of the master hand's thumb and $q_{\inf}$ and $q_{\sup}$ are the related inferior

and superior joint limits, respectively. In this relation, we can consider the forward kinematics function of the thumb $\mathcal{F}_T : Q_T \subset \mathbb{R}^n \to \mathbb{R}^3$. We therefore define the workspace of the master hand's thumb as

$$W_T = \left\{ {}^M p_T \in \mathbb{R}^3 : {}^M p_T \in \mathcal{F}_T(Q_T) \right\}, \qquad (2)$$

that is, the set of all thumb fingertip Cartesian positions reachable within joint limits. Let us also refer to the workspace of the master's index finger as the set W_I, defined in an analogous manner as for the thumb, i.e. considering the set of index admissible joint configurations Q_I and the index forward kinematics $\mathcal{F}_I(\bullet)$. We can therefore consider the region of the master hand's workspace in which the thumb and index fingertips can get in contact as

$$C_{TI} = W_T \cap W_I. \qquad (3)$$

In the context of our mapping algorithm, we are interested in approximating the region C_{TI} as the convex hull of a point cloud that discretizes C_{TI} itself. Indeed, we can consider a finite set of points taken from a discretization of the Cartesian space as

$$D = \left\{ [x\ y\ z]^T \in \mathbb{R}^3 : \begin{cases} x = 0d, 1d, 2d, \ldots, ld \\ y = 0d, 1d, 2d, \ldots, hd \wedge d \in \mathbb{R} \\ z = 0d, 1d, 2d, \ldots, kd \end{cases} \right\}, \qquad (4)$$

with uniform granularity d, and $l, k, h \in \mathbb{N}$ such that $D \supseteq (W_T \cup W_I)$. This allows us to practically compute a point cloud discretizations of W_T and W_I, defined as $D_T = W_T \cap D$ and $D_I = W_I \cap D$, respectively, by simply applying the thumb and index inverse kinematic functions $\mathcal{I}_T(\bullet)$ and $\mathcal{I}_I(\bullet)$ to D[1]. More specifically, we impose that

$$D_T = \{ d_T \in D : \mathcal{I}_T(d_T) \in Q_T \ \wedge \ \mathcal{F}_T(\mathcal{I}_T(d_T)) = d_T \}, \\ D_I = \{ d_I \in D : \mathcal{I}_I(d_I) \in Q_I \ \wedge \ \mathcal{F}_I(\mathcal{I}_T(d_I)) = d_I \}. \qquad (5)$$

The point cloud discretization of C_{TI} then directly follows as

$$P_{TI} = D_T \cap D_I. \qquad (6)$$

Therefore, it is now possible to compute the convex hull of the point cloud P_{TI}. The reason of our interest to this lies in the fact that convex hulls present convenient topological features, such as they can be easily and uniformly scaled/offsetted by simply applying a multiplying factor to each Cartesian dimension without the risk of generating self-intersecting regions, which instead is non-trivial with non-convex polyhedra. We exploit the properties of convex hulls in our method, as subsequently reported. Recalling now the definition of convex set from linear algebra, a set $S \subseteq \mathbb{R}^{\dim}$ is convex if it satisfies that for every line $t \subseteq \mathbb{R}^{\dim}$ the intersection $t \cap S$ is connected. It follows that the master hand's convex hull ${}^M H$ of the point cloud P_{TI} of N points is the

---

[1]We consider that kinematic inversion is obtained by means of an iterative, gradient-based optimization method, therefore applicable to any point of the Cartesian space [20].
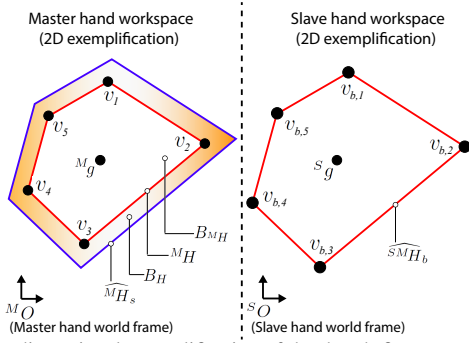
Fig. 2. Two-dimensional exemplification of the thumb-finger convex hulls for the master and slave hands. The notation is with respect to Subsecs. II-A, II-B, II-C.

intersection of all convex sets containing P_{TI} [21], and is given by the expression

$$^{M}H = \left\{ \sum_{i=1}^{N} a_{i} p_{i} : p_{i} \in P_{TI} \wedge a_{i} \geq 0 \wedge \sum_{i=1}^{N} a_{i} = 1 \right\}. \tag{7}$$

A 2-dimensional graphical exemplification of this convex hull is illustrated on the left side of Fig. 2.

Once the convex hull ^{M}H is given, it is possible to consider the continuous set $B_{MH} \supseteq {}^{M}H$ containing the points of the hand workspace region delimited by ^{M}H, and its discretization $D_{MH} = D \cap B_{MH}$. Then, we compute the centroid ^{M}g of ^{M}H as

$$^{M}g = \frac{\sum_{i=1}^{n_{V}} v_{i}}{n_{V}}, \tag{8}$$

where $v_{i} \in D_{MH}$ (see also Fig. 2) and n_{V} is the number of elements of D_{MH}.

B. Joint-Cartesian Mapping Transition

Continuing considering only the thumb and index finger without loss of generality, in the proposed method we want to realize that a master-to-slave Cartesian mapping is in place when both index and thumb fingertips are inside the hand workspace region delimited by the convex hull ^{M}H, i.e. the set of points $B_{MH} \supseteq {}^{M}H$, whereas outside such region a joint mapping is enforced. It follows that also the definition of a transition region between the two kinds of mapping needs to be introduced.

Considering the centroid ^{M}g given by eq. (8), let $\widehat{^{M}H}_{s}$ be the scaling of the convex hull ^{M}H by a scale factor s, which can be formally described as

$$\widehat{^{M}H}_{s} = \left\{ h_{s,i} = s(h_{i} - {}^{M}g) + {}^{M}g : h_{i} \in {}^{M}H \wedge s \in \mathbb{R}^{+} \right\}. \tag{9}$$

Consequently, $B_{\widehat{^{M}H}_{s}}$ will denote the region of the master hand workspace delimited by $\widehat{^{M}H}_{s}$. We also define the set $B_{H} = B_{\widehat{^{M}H}_{s}} \setminus B_{MH}$, containing all the hand workspace points corresponding to $B_{\widehat{^{M}H}_{s}}$ that does not belong to B_{MH}. On the left side of Fig. 2 it is possible to observe a graphical 2-dimensional exemplification of $\widehat{^{M}H}_{s}$ and B_{H}.

Now, taking a $\widehat{^{M}H}_{s}$ with $s > 1$ (in our implementation we chose $s = 1.2$, see Sec. III), we consider a function, named *transition*,

$$f : B_{H} \subset \mathbb{R}^{3} \to \mathbb{R} \tag{10}$$

linearly interpolating the nodes $(h_{s,i}, 0)$ and $(h_{i}, 1)$ (according to the notation of eq. (9).) Therefore, in this way we obtain: *(i)* a transition $f(h_{s,i}) = 0, \forall\, h_{s,i} \in \widehat{^{M}H}_{s}$, *(ii)* a transition $f(h_{s,i}) = 1, \forall\, h_{s,i} \in {}^{M}H$ and *(iii)* linearly interpolated values of transition for any remaining point of the domain $Dom(f) = B_{H}$. We solve this multidimensional interpolation problem as a radial basis function (RBF) interpolation problem [22], in particular computing the interpolant function f as a weighted sum of linear radial basis functions (we refer the reader to [22] for RBF and RBF interpolation details.) It is therefore possible to consider, for the master hand, a *thumb transition* $f_{T} = f(^{M}p_{T})$ and an *index transition* $f_{I} = f(^{M}p_{I})$, where $^{M}p_{T}$ and $^{M}p_{I}$ are the Cartesian position of the thumb and index fingertips, respectively. Finally, we define the *thumb-index transition* function $f_{TI}(f_{T}, f_{I})$, or simply f_{TI}, as

$$f_{TI}(f_{T}, f_{I}) = \begin{cases} f_{T}, & \text{if } f_{T} \leq f_{I} \\ f_{I}, & \text{if } f_{T} > f_{I} \end{cases}. \tag{11}$$

Eq. (11) allows us to have a transition value belonging to the interval $[0,1]$ without discontinuities for all $^{M}p_{T}, {}^{M}p_{I} \in B_{H}$.

We therefore exploit the transition function f_{TI} to pass from joint to Cartesian mapping and vice versa. Let us put in the case of joint mapping. Joint and Cartesian mappings can present differences based on specific implementation choices, but we do not consider this aspect now, since in Subsec. II-D and II-C we report our specific implementations. Instead, we here stick to the general case, and therefore we just consider that, during joint mapping, the slave hand joint values for the thumb and index finger $^{S}q_{T,Q}$ and $^{S}q_{I,Q}$ are given, since they are directly available from the master hand (the left superscript "^{S}" indicates the slave hand, also in the following.) It follows that we can apply the slave hand forward kinematics to compute the Cartesian positions $^{S}p_{T,Q}$, $^{S}p_{I,Q}$ and orientations $^{S}o_{T,Q}, {}^{S}o_{I,Q}$ of the thumb and index fingertips, respectively, as resulting from the application of the joint mapping. $^{S}o_{T,Q}$ and $^{S}o_{I,Q}$ can be any suitable representation of the fingertips orientations, such as Euler angles or unit quaternion. Therefore, collecting the Cartesian position and orientation in a single fingertip pose vector for both thumb and index

$$^{S}x_{T,Q} = \begin{bmatrix} {}^{S}p_{T,Q} \\ {}^{S}o_{T,Q} \end{bmatrix} \quad \text{and} \quad {}^{S}x_{I,Q} = \begin{bmatrix} {}^{S}p_{I,Q} \\ {}^{S}o_{I,Q} \end{bmatrix}, \tag{12}$$

from the application of the forward kinematic results that $^{S}x_{T,Q} = {}^{S}\mathcal{F}_{T}(^{S}q_{T,Q})$ and $^{S}x_{I,Q} = {}^{S}\mathcal{F}_{I}(^{S}q_{I,Q})$. Similarly, if we put in the case of Cartesian mapping, we consider that the thumb and index fingertip poses $^{S}x_{T,C}$ and $^{S}x_{I,C}$ are available, according to the notation

$$^{S}x_{T,C} = \begin{bmatrix} {}^{S}p_{T,C} \\ {}^{S}o_{T,C} \end{bmatrix} \quad \text{and} \quad {}^{S}x_{I,C} = \begin{bmatrix} {}^{S}p_{I,C} \\ {}^{S}o_{I,C} \end{bmatrix}, \tag{13}$$

where $^{S}p_{T,C}$, $^{S}p_{I,C}$ are the Cartesian positions and $^{S}o_{T,C}$, $^{S}o_{I,C}$ the orientations of the slave thumb and index fingertips, respectively, as directly available from the application of the Cartesian mapping.

Then, referring to the generic slave hand thumb and index finger joint values as $^{S}q_{I}$ and $^{S}q_{T}$, respectively, it is possible to

think them as given by the related inverse kinematics functions as

$$
\begin{aligned}
{}^S q_T &= {}^S\mathcal{I}_T({}^S x_{T,input}), \\
{}^S q_I &= {}^S\mathcal{I}_I({}^S x_{I,input}),
\end{aligned}
\tag{14}
$$

with

$$
x_{T,input} = \begin{bmatrix} {}^S p_{T,input} \\ {}^S o_{T,input} \end{bmatrix} \quad \text{and} \quad x_{I,input} = \begin{bmatrix} {}^S p_{I,input} \\ {}^S o_{I,input} \end{bmatrix}, \tag{15}
$$

and where ${}^S p_{T,input}, {}^S p_{I,input}$ and ${}^S o_{T,input}, {}^S o_{I,input}$ are thumb and index Cartesian position and orientation inputs, respectively. We therefore impose, according to our mapping approach, that for the position inputs

$$
\begin{aligned}
{}^S p_{T,input} &= (1 - k_{TI})\,{}^S p_{T,Q} + k_{TI}\,{}^S p_{T,C}, \\
{}^S p_{I,input} &= (1 - k_{TI})\,{}^S p_{I,Q} + k_{TI}\,{}^S p_{I,C},
\end{aligned}
\tag{16}
$$

where k_{TI} is a smooth, sigmoidal gain described by

$$
k_{TI} = \begin{cases} 0 & \text{if } {}^M p_T, {}^M p_I \notin B_{\widehat{\overline{M}H_s}} \\ 1, & \text{if } {}^M p_T, {}^M p_I \in B_{M_H} \\ \frac{1}{2}(1 - \cos(\pi f_{TI})) & \text{if } {}^M p_T, {}^M p_I \in B_H \end{cases}. \tag{17}
$$

Instead, for the orientation input we impose $o_{T,input} = o_{T,map}$ and $o_{I,input} = o_{I,map}$, where

$$
o_{T,map} = \begin{cases} {}^S o_{T,Q} & \text{if } k_{TI} = 0 \\ {}^{SM} o_T & \text{otherwise} \end{cases}, \tag{18}
$$

$$
o_{I,map} = \begin{cases} {}^S o_{I,Q} & \text{if } k_{TI} = 0 \\ {}^{SM} o_I & \text{otherwise} \end{cases}, \tag{19}
$$

where $o_{T,Q}$ and $o_{I,Q}$ are from eq. (12), whereas ${}^{SM} o_T$ and ${}^{SM} o_I$ are the orientations of master thumb and index fingertips with respect to the master finger base reference frames, consistently described with respect to the slave index and thumb base reference frames[2]. Specifically, let ${}^M R_{o_I}$ and ${}^M R_{o_T}$ be the rotation matrices – with respect to the related master finger base frames – associated to the index and thumb fingertip orientations o_I and o_T, respectively. Then, ${}^{SM} o_I$ and ${}^{SM} o_T$, in eq. (19), will be the orientations of master index and thumb – with respect to the related slave finger base frames – associated to the rotation matrices ${}^{SM} R_{o_I} = R_{SM_I}\,{}^M R_{o_I}$ and ${}^{SM} R_{o_T} = R_{SM_T}\,{}^M R_{o_T}$, respectively, where R_{SM_I} and R_{SM_T} compensate for different orientation of slave base-frames/fingertips with the respect to the master when the hands are in home configuration (i.e. when joints angles are zero, see Fig. 4). The general scheme of the mapping algorithm can be observed in Fig. 3.

Eqs. (16)—(17) allow to have a smooth transition, with a spatial sigmoid-like profile and without discontinuities, from joint to Cartesian mapping and vice versa for the slave hand thumb and index. If ${}^M p_T$ and ${}^M p_I$ are located in the master hand's workspace region delimited by the convex hull ${}^M H$, a Cartesian mapping is enforced, whereas a joint mapping is

imposed if ${}^M p_T$ and ${}^M p_I$ are outside of the region delimited by $\widehat{{}^M H_s}$. Finally, a transition takes place when both the master thumb and index fingertips cross the transition region corresponding to the set of points B_H, following eqs. (16). Note that, according to Fig. 3 and eq. (16), the transition is performed in Cartesian space (instead that in joint space.) This solution ensures a linear motion of the fingertip during the transition between the configurations computed from joint mapping and from Cartesian mapping, which results in a more predictable behaviour of the slave hand.

C. Cartesian Mapping

Referring to eq. (7), let's now consider again, in relation to the master hand, the convex hull ${}^M H$ and its centroid ${}^M g$, which are implicitly considered as described with respect to a master hand's world reference frame ${}^M O$–xyz (i.e., the reference frame with origin ${}^M O$ and orthogonal axes x, y and z) or, more compactly, the reference frame denoted by $\{{}^M O\}$. Differently, we define ${}^M H^*$ and ${}^M g^*$ as the description of ${}^M H$ and ${}^M g$ with respect to a new reference frame $\{{}^M G\}$, the origin of which is placed in ${}^M g$, the plane with y and z parallel to the master hand index's frontal plane, and the plane with x and z axes parallel to the master hand index's sagittal median plane (refer to Fig. 1.) In this relation, T_{MG} denotes the homogeneous transformation matrix that describes $\{{}^M G\}$ with respect to $\{{}^M O\}$. We are going to use this in a moment.

Let's now consider the slave hand. We can repeat the same procedure —considering only the thumb and index finger without loss of generality— described by the eqs. (2)—(8), and therefore consider for the slave hand a convex hull ${}^S H$ with centroid ${}^S g$. We are here just interested in ${}^S g$. In particular, we place in ${}^S g$ a reference frame $\{{}^S G\}$ such that the plane formed by its y and z axes is parallel to the slave hand index's frontal plane, and the plane formed by x and z axes is parallel to the slave hand index's sagittal median plane (in a specular way as for the master hand, see also Fig. 1.) Therefore, it is possible to consider the convex hull ${}^S H^*$, corresponding to ${}^S H$ described with respect to $\{{}^S G\}$. The related homogeneous matrix transformation describing $\{{}^S G\}$ with respect to the slave hand world frame $\{{}^S O\}$ is denoted by $T_{{}^S G}$. It is possible now to consider the convex hull ${}^{SM} H^*$, corresponding to the points of ${}^M H^*$ placed in the slave hand workspace and imposed as described with respect to $\{{}^S G\}$. We also directly introduce the set ${}^{SM} H$ as the description of ${}^{SM} H^*$ with respect to the slave hand world frame $\{{}^S O\}$. The latter is nothing more than the master hand convex hull directly placed in ${}^S g$. Furthermore, we are also interested in applying a scaling to ${}^{SM} H$, given by

$$
\widehat{{}^{SM} H}_b = \left\{ h_{b,i} = b(h_i - {}^S g) + {}^S g : h_i \in {}^{SM} H \wedge b \in \mathbb{R}^+ \right\}, \tag{20}
$$

where the scaling factor b is chosen such that

$$
max(|\hat{x}|)\big|_{[\hat{x}\ \hat{y}\ \hat{z}]^T \in \widehat{{}^{SM} H^*}_b} = max(|x|)\big|_{[x\ y\ z]^T \in {}^S H^*}, \tag{21}
$$

where $\widehat{{}^{SM} H^*}_b$ is the description of $\widehat{{}^{SM} H}_b$ with respect to $\{{}^S G\}$. In other words, eq. (21) means that the scaling factor b

---

[2]We consider that inverse kinematics solutions are obtained by means of iterative, gradient-based optimization methods in which the position target can be prioritized with respect to the orientation target, allowing an admissible orientation with the smallest joint deviation when the imposition of the master hand orientation is not compatible with the position [20].
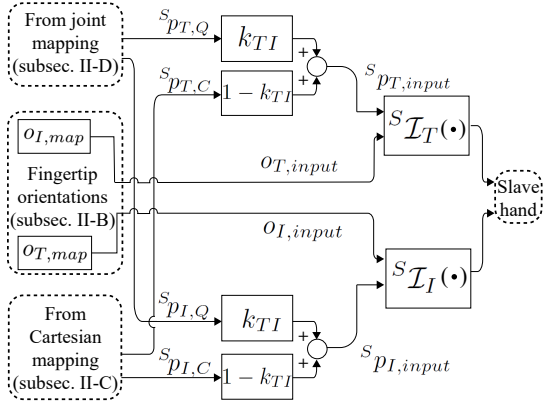
Fig. 3. Block diagram of the proposed hybrid joint-Cartesian mapping algorithm.

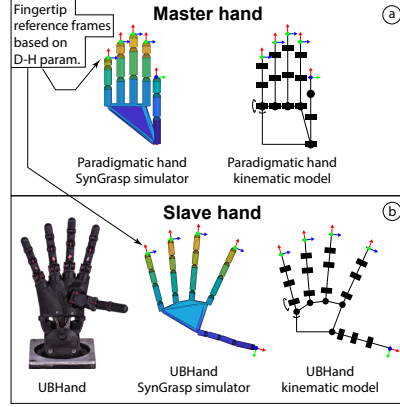

Fig. 4. (a) Master hand (paradigmatic hand) and (b) slave hand (UBHand.)

Fig. 5. (a)-(b) Thumb-index convex hulls.(c)-(d) All convex hulls.

is chosen such that the maximum extension of $\widehat{SMH^*}_b$ along the x axis (in absolute value) matches the maximum extension along the x axis (in absolute value) of $^SH^*$. This allows that the range of values of $^SH^*$ along the x axis are contained within the range of values of $\widehat{SMH^*}_b$. This is important for the proposed mapping, because the x axis of $\{^SG\}$ indicates the distance from the palm. Refer to Fig. 2 for a 2-dimensional graphical exemplification of $\widehat{SMH}_b$ and of the other convex hulls considered.

After the steps described until now, it is possible to impose a Cartesian mapping as follows. We denote by $^{SM}p_T$ and $^{SM}p_I$ the position of the master thumb and index fingertips ^Mp_T and ^Mp_I such that they are: *(i)* written with respect to the frame $\{^MG\}$, then *(ii)* imposed to the slave hand with respect to the frame $\{^SG\}$, and finally *(iii)* described with respect to the world frame $\{^SO\}$. Formally, $^{SM}p_T$ and $^{SM}p_I$ are given as

$$
\begin{aligned}
^{SM}p_T &= T_{^SG} \ (T_{^MG})^{-1} \ ^Mp_T, \\
^{SM}p_I &= T_{^SG} \ (T_{^MG})^{-1} \ ^Mp_I.
\end{aligned}
\tag{22}
$$

Then, the Cartesian position of the slave hand thumb and index fingertips $^Sp_{T,C}$ and $^Sp_{I,C}$ will be imposed as

$$
\begin{aligned}
^Sp_{T,C} &= b(^{SM}p_T - \,^Sg) + \,^Sg, \\
^Sp_{I,C} &= b(^{SM}p_I - \,^Sg) + \,^Sg,
\end{aligned}
\tag{23}
$$

where the notation is relative also to eqs. (21) and (22). In this way, $^Sp_{T,C}$ and $^Sp_{I,C}$ are available for the eqs. (16), the latter describing the general transition between joint and Cartesian mappings of the hybrid approach proposed in this work. Now, the joint mapping remains to be illustrated, as follows in the next subsection.

D. Joint Mapping

Let's consider the vector of joint angles of thumb and index finger for both the master hand (^Mq_T and ^Mq_I) and slave hand (^Sq_T and ^Sq_I) as

$$
\begin{aligned}
^Sq_T &= [\,^Sq_{T,1} \quad ^Sq_{T,2} \cdots \quad ^Sq_{T,i} \cdots \quad ^Sq_{T,m}]^T, \\
^Sq_I &= [\,^Sq_{I,1} \quad ^Sq_{I,2} \cdots \quad ^Sq_{I,j} \cdots \quad ^Sq_{I,l}]^T, \\
^Mq_T &= [\,^Mq_{T,1} \quad ^Mq_{T,2} \cdots \quad ^Mq_{T,h} \cdots \quad ^Mq_{T,n}]^T, \\
^Mq_I &= [\,^Mq_{I,1} \quad ^Mq_{I,2} \cdots \quad ^Mq_{I,k} \cdots \quad ^Mq_{I,p}]^T,
\end{aligned}
$$

where m, l, n, p are the number of joints of the slave thumb, slave index, master thumb and master index, respectively. We therefore define the joint mapping —for the only thumb and index finger without loss of generality— as

$$
\begin{aligned}
^Sq_{T,i} &= \,^Mq_{T,h}, \text{ with } i = 1, 2, \ldots, m \wedge \forall i, h \in \{1, 2, \ldots, n\} \\
^Sq_{I,j} &= \,^Mq_{I,k}, \text{ with } j = 1, 2, \ldots, l \wedge \forall j, k \in \{1, 2, \ldots, p\},
\end{aligned}
\tag{24}
$$

and where h and k are chosen empirically for each i-th and j-th component of ^Sq_T and ^Sq_I, respectively. Thereafter, by applying the forward kinematics function of the slave hand thumb and index finger, it is possible to obtain the relative Cartesian positions $^Sp_{T,Q}$ and $^Sp_{I,Q}$ that come from the joint mapping as

$$
\begin{aligned}
^Sp_{T,Q} &= \,^S\mathcal{F}_T(^Sq_T), \\
^Sp_{I,Q} &= \,^S\mathcal{F}_I(^Sq_I).
\end{aligned}
\tag{25}
$$

In this way, $^Sp_{T,Q}$ and $^Sp_{I,Q}$ are computed and can be used within eqs. (16), which describe the general transition between joint and Cartesian mappings.

III. Experimental Evaluation

In order to evaluate the proposed hand mapping, we used as master hand a simulated robotic hand, the *paradigmatic hand model* (Fig. 4) available from the open-source SynGrasp Matlab toolbox [23]. As slave hand we used the University of Bologna Hand IV (UBHand), a fully-actuated anthropomorphic robotic hand developed at our laboratory [24] (Fig. 4.). Note that, looking at Fig. 4, it possible to observe the fingertip reference frames, which are exactly placed at the end of the semi-spherical tip of the last finger phalanx, in the same way for master and slave. The definition of fingertip reference frames is based on the standard Denavit-Hartenberg (D-H) convention (for details on the specific D-H parameters see [23] for the paradigmatic hand, and [24] for the UBHand.)

For the specific implementation of the mapping algorithm we have chosen the value of the parameters of granularity of the workspace discretization $d = 1\text{mm}$ and scaling factor $s = 1.2$ for the thumb-finger convex hull $\widehat{MH}_s$. We arbitrarily chose s=1.2 because it resulted as a good value for preserving as much workspace as possible for the joint mapping, without
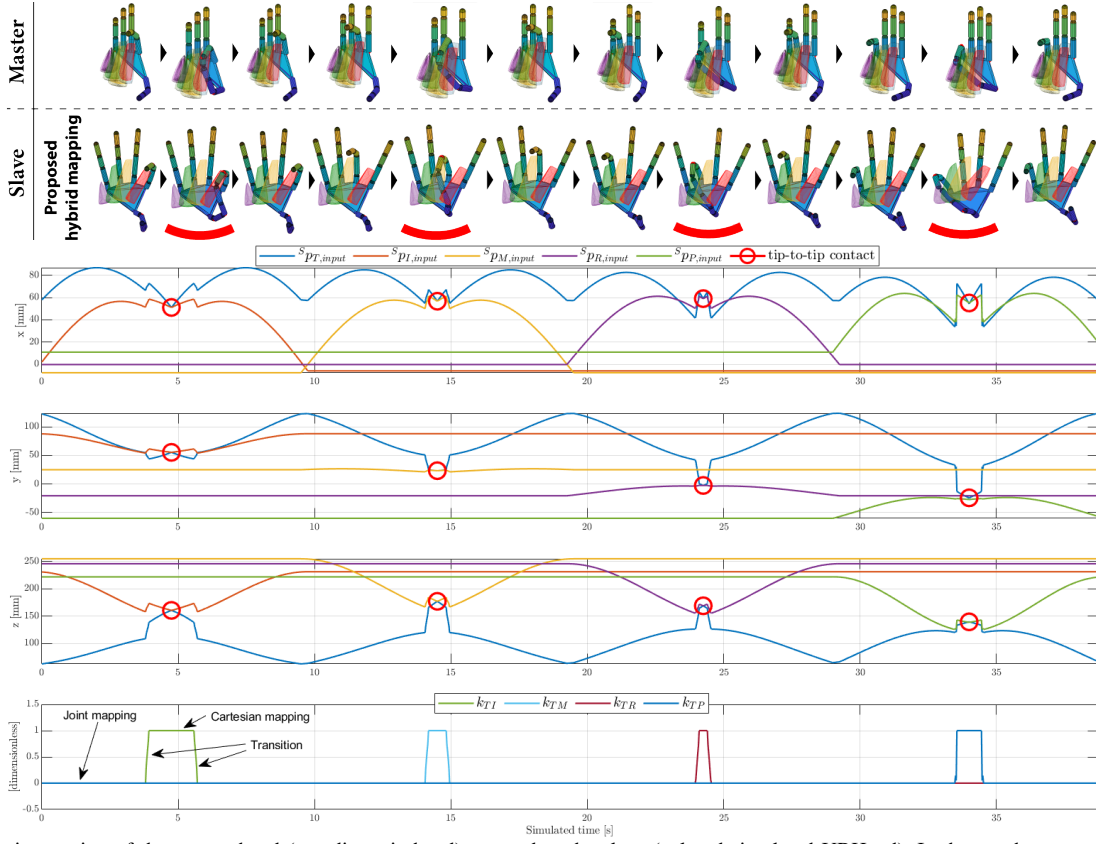
Fig. 6. Tips-to-tips motion of the master hand (paradigmatic hand) mapped to the slave (colored simulated UBHand). In the graph, x, y and z denotes the components of $^{S}p_{T,input}$, $^{S}p_{I,input}$, $^{S}p_{M,input}$, $^{S}p_{R,input}$ and $^{S}p_{P,input}$, which are the slave fingertip positions of thumb, index, middle, ring and pinkie fingers, respectively. Both in the top master-slave hand visualization and in the graphs, the moments of tip-to-tip contacts are highlighted with red lines and circles.

having too abrupt transitions. The convex hull centroids ^{M}g and ^{S}g can be observed in Fig. 5(a)-(b) for the index finger, along with the related reference frames $\{^{M}G\}$ and $\{^{S}G\}$. The implemented Cartesian mapping part of the hybrid mapping is described in Subsec. II-C, and the joint mapping part imposes the angle values of the master to the slave hand, since they have the same number of joints for each finger, in accordance with the description of Subsec. II-D.

1) Simulation experiment: Master and slave hands are shown in Fig. 5 along with the convex hulls. In Fig. 5(a)-(b), it is possible to see the thumb-index convex hull ^{M}H, that defines the master hand workspace area for which a Cartesian mapping is enforced (see eqs. (16)). Also, it is possible to observe the related scaled convex hull $\widehat{^{M}H_{s}}$ (according to eq. (20), with a scaling factor $s = 1.2$) that is used to define the transition zone between joint and Cartesian mappings. The approach can be easily extended for all thumb-finger pairs, as illustrated in Fig. 5(c)-(d). In particular, a motion of the hand master has been generated, consisting in starting from the configuration with all fingers completely extended, and performing motions such that all thumb-finger fingertips get in contact once at a time in a sequence, as can be seen in Fig. 6, reporting the master-slave hand visualization and graphs of slave fingertips positions and gains for joint-Cartesian mapping transitions. In Fig. 6, it can be observed that the slave hand conserves the shape of the master hand fingers that are not close —in the sense of the thumb-finger convex hull— to the thumb, since they are mapped with joint

mapping. At the same time, the thumb-finger fingertips get correctly in contact when such contact occurs on the master side, since in that area of the master hand workspace (i.e., inside the convex hull concerned) the Cartesian mapping is applied. The transitions from joint to Cartesian mappings can be appreciated in the bottom plot, in which the behaviour of the gains k_{TI}, k_{TM}, k_{TR} and k_{TP} is reported, related to the slave index, middle, ring and pinkie fingers, respectively. The motion reported in Fig. 6 have been realized by a Matlab implementation of the proposed hybrid mapping, and a version of the code has been released in the GitHub repository: https://github.com/TipeaTapei/HybridHandMapping.

2) Comparison with other mappings: The comparison is performed between the proposed method and: *(i)* a standard, full direct joint mapping in accordance with Speeter et al. [8], *(ii)* a standard, full direct Cartesian mapping as presented by Rohling et al. [6], and *(iii)* a virtual-object-based mapping [12]. In Fig. 7 we have divided the motion illustrated in Fig. 6 in its four thumb-finger submovements starting from the open hand posture, passing through the tip-to-tip contact, and coming back to the open hand. We have applied the three mappings and the proposed hybrid mapping for each submotion, and computed two metrics: the *shape error*, that is the norm of the error between the joint angle vectors of the master and the slave, and the norm of the *thumb-finger fingertip distance error* between master and slave, the latter related to a different specific finger in each considered submotion. The errors were computed independently for each sub-motion, and
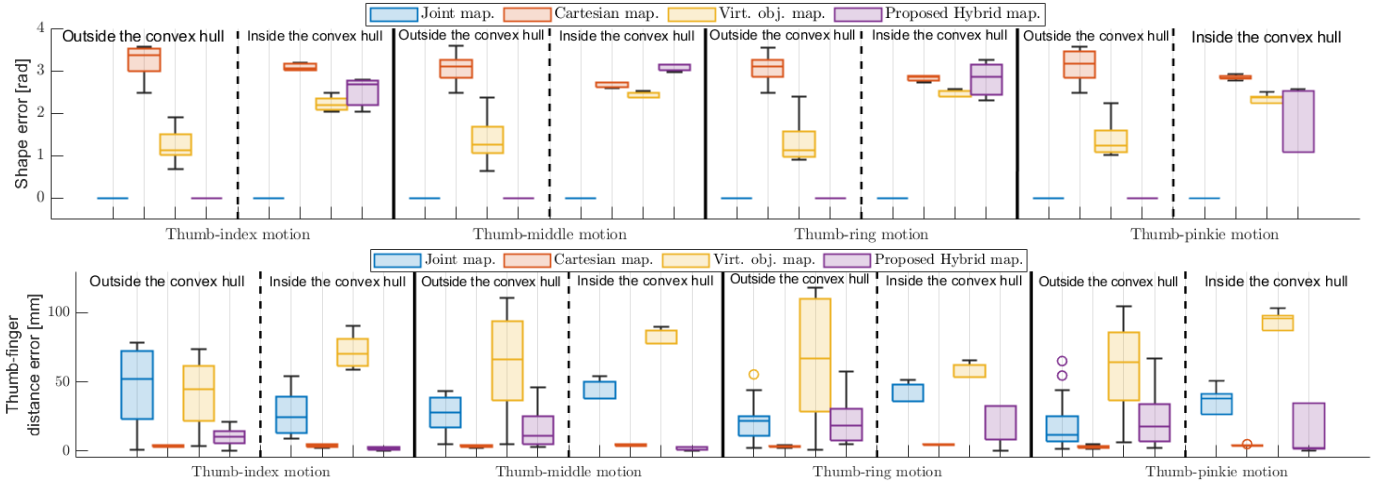
Fig. 7. Comparison of the proposed hybrid mapping with standard direct joint [8], standard Cartesian [6] and virtual object [12] mappings.
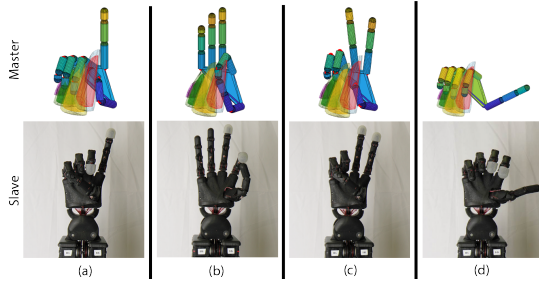

Fig. 8. Gestures mapped on the real UBHand. (a) "Index pointing", (b) "O.K.", (c) "V for victory" and (d) "thumb up".
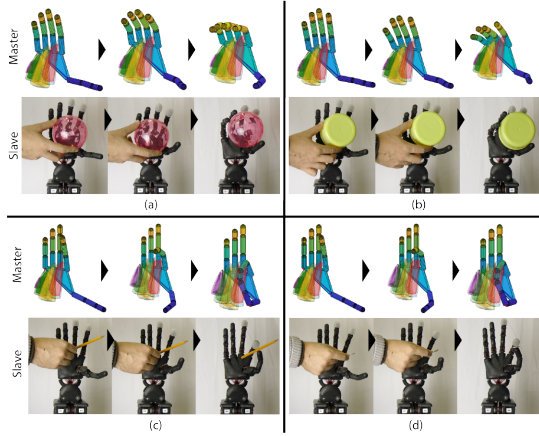

Fig. 9. Mapping of grasps on the real UBHand. (a) Large ball and (b) large cylinder. (c) Pencil and (d) coin.
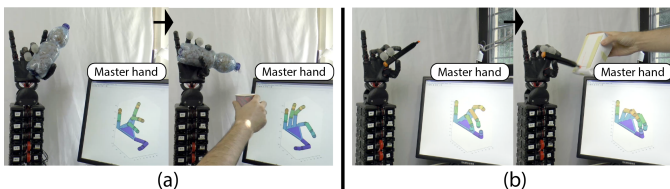

Fig. 10. (a) Volar grasp application: pouring mock-up liquid from a bottle. (b) Precision grasp application: drawing a line with a marker.

the motion was discretized in 8000 configurations, uniformly distributed in joint space with respect to the master hand. As can be observed in the top graph of Fig. 7, outside of the master convex hulls the proposed hybrid mapping (purple) completely conserves the master shape on the slave hand, as also happens for the standard joint mapping (blue), since in such case they produce the same behaviour. Standard Cartesian (red) and virtual object (yellow) mappings show clear shape discrepancies outside of the convex hull. Differently, for motions inside the convex hull, the hybrid mapping presents an increment of the shape error, however in an order of magnitude comparable with the Cartesian and virtual object ones. This is obtained thanks to the meaningful scaling and orientation of the convex hulls within the slave hand. Looking now at the bottom graph of Fig. 7, it is possible to see how – within the considered context of the master motions inside the convex hull – the hybrid mapping presents some zero thumb-finger fingertip errors (lower whisker of the boxplots), being capable of totally overcoming the kinematic dissimilarities between master and slave. Even the standard Cartesian mapping, which directly provides the actual thumb-fingers distance to the slave hand, doesn't show any zero value distance error, due to the fact that the imposed positions cannot actually be reached by the slave hand. This latter limitation, is again compensated by the convex hulls scaling and orientation of the hybrid mapping. Then, especially for the motions outside of the convex hulls, it is possible to observe high values of thumb-finger distance errors for the virtual object mapping, which shows a clear difficulty in reproducing precision bi-digital grasps. Generally, it works better for shape preservation. Also outside of the convex hull, the hybrid mapping shows reasonable limited thumb-finger distance errors, by virtue of an optimum shape preservation. Conversely, standard Cartesian mapping presents very low distance errors for all motions, but at the cost of very high shape error values during the entire execution of the tips-to-tips motion.

3) Test with the real UBHand: We tested the mapping using the real UBHand as slave robotic hand, as reported in Fig. 8, Fig. 9 and Fig. 10. Note that, also in this experiment, the master hand was simulated, and its predefined motions were

directly mapped to the real slave hand using the proposed method. Referring to Fig. 8, we first tested the mapping of a series of hand gestures performed by the master hand. In particular, the gestures are: "index pointing", "O.K.", "V for Victory" and "thumbs up". As can be observed in the figure,it is clear the meaningful reproduction of the gestures on the slave hand. Referring now to Fig. 9, it can be observed the grasping of a series of objects with the UBHand. Specifically, we have carried out: *(i)* two volar grasps (objects "large ball" and "large cylinder") and *(ii)* two precision grasps (objects "pencil" and "coin"). Finally, Fig. 10 shows video frames during the performance of a volar grasp application (pouring of mock-up liquid from a bottle, see Fig. 10(a)) and a precision grasp application (drawing a line with a marker, Fig. 10(b)). From the reported tests it is possible to see that the proposed hybrid mapping allows a hand mapping which is able of performing transitions between joint mapping for shape preservation and volar grasp execution, and Cartesian mapping for correct tip-to-tip contacts and precision grasps.

4) Real-time performance: Finally, we also performed a qualitative evaluation of the frequency at which it was possible to compute the slave hand joint values – given the master hand joint values – over the motion reported in Fig. 6 (i.e., over 8000 cycles) using the proposed mapping. In particular, we observed a mean frequency of 136.98 Hz with a standard deviation of 69.87 Hz (system features: processor 64 bit, Intel Core i7-6700 CPU @ 3.40GHz x 8, 32GB RAM, ubuntu 18.04, Kinematics and Dynamics Library (KDL) from Orocos.) Therefore, considering 50 Hz as a reasonable minimum frequency for real-time position control, the proposed mapping algorithm can be applied in real-time.

IV. CONCLUSIONS

In this article a hybrid joint-Cartesian mapping based on in-hand knowledge of the master and slave hands has been proposed for anthropomorphic robotic hands. Tests and comparisons have been performed both in simulation and with a real anthropomorphic hand, showing the successful preservation of master finger shapes and correctness of slave fingertips mapping. Future developments will explore the possibility of varying the shapes of the computed thumb-finger convex hulls in an on-line fashion. Furthermore, in the studies related to future developments, we want to apply multiple mapping methods with the real robotic hand for comparison purposes, also testing different master and slave hands, whereas in the present study, the focus was on proposing the novel mapping approach and more attention was devoted to comparisons performed in simulation using the paradigmatic and UBHand hands.

REFERENCES

[1] M. Shahbazi, S. F. Atashzar, and R. V. Patel, "A systematic review of multilateral teleoperation systems," *IEEE transactions on haptics*, vol. 11, no. 3, pp. 338–356, 2018.

[2] R. N. Rohling, J. M. Hollerbach, and S. C. Jacobsen, "Optimized fingertip mapping: a general algorithm for robotic hand teleoperation," *Presence: Teleoperators & Virtual Environments*, vol. 2, no. 3, pp. 203–220, 1993.

[3] M. Bianchi, P. Salaris, and A. Bicchi, "Synergy-based hand pose sensing: Optimal glove design," *The International Journal of Robotics Research*, vol. 32, no. 4, pp. 407–424, 2013.

[4] A. Erol, G. Bebis, M. Nicolescu, R. D. Boyle, and X. Twombly, "A review on vision-based full dof hand motion estimation," in *2005 IEEE Computer Society Conference on Computer Vision and Pattern Recognition (CVPR'05)-Workshops*. IEEE, 2005, pp. 75–75.

[5] M. Bergamasco, A. Frisoli, and C. A. Avizzano, "Exoskeletons as man-machine interface systems for teleoperation and interaction in virtual environments," in *Advances in Telerobotics*. Springer, 2007, pp. 61–76.

[6] R. N. Rohling and J. M. Hollerbach, "Optimized fingertip mapping for teleoperation of dextrous robot hands," in *[1993] Proceedings IEEE International Conference on Robotics and Automation*. IEEE, 1993, pp. 769–775.

[7] L. Colasanto, R. Suárez, and J. Rosell, "Hybrid mapping for the assistance of teleoperated grasping tasks," *IEEE Transactions on Systems, Man, and Cybernetics: Systems*, vol. 43, no. 2, pp. 390–401, 2012.

[8] T. H. Speeter, "Transforming human hand motion for telemanipulation," *Presence: Teleoperators & Virtual Environments*, vol. 1, no. 1, pp. 63–79, 1992.

[9] I. Cerulo, F. Ficuciello, V. Lippiello, and B. Siciliano, "Teleoperation of the schunk s5fh under-actuated anthropomorphic hand using human hand motion tracking," *Robotics and Autonomous Systems*, vol. 89, pp. 75–84, 2017.

[10] R. N. Rohling and J. M. Hollerbach, "Calibrating the human hand for haptic interfaces," *Presence: Teleoperators & Virtual Environments*, vol. 2, no. 4, pp. 281–296, 1993.

[11] R. Chattaraj, B. Bepari, and S. Bhaumik, "Grasp mapping for dexterous robot hand: A hybrid approach," in *2014 Seventh International Conference on Contemporary Computing (IC3)*. IEEE, 2014, pp. 242–247.

[12] G. Gioioso, G. Salvietti, M. Malvezzi, and D. Prattichizzo, "Mapping synergies from human to robotic hands with dissimilar kinematics: an approach in the object domain," *IEEE Transactions on Robotics*, vol. 29, no. 4, pp. 825–837, 2013.

[13] G. Salvietti, M. Malvezzi, G. Gioioso, and D. Prattichizzo, "On the use of homogeneous transformations to map human hand movements onto robotic hands," in *2014 IEEE International Conference on Robotics and Automation (ICRA)*. IEEE, 2014, pp. 5352–5357.

[14] C. Meeker, T. Rasmussen, and M. Ciocarlie, "Intuitive hand teleoperation by novice operators using a continuous teleoperation subspace," in *2018 IEEE International Conference on Robotics and Automation (ICRA)*. IEEE, 2018, pp. 1–7.

[15] S. Ekvall and D. Kragic, "Interactive grasp learning based on human demonstration," in *IEEE International Conference on Robotics and Automation, 2004. Proceedings. ICRA'04. 2004*, vol. 4. IEEE, 2004, pp. 3519–3524.

[16] L. M. Pedro, G. A. Caurin, V. L. Belini, R. D. Pechoneri, A. Gonzaga, I. Neto, F. Nazareno, and M. Stücheli, "Hand gesture recognition for robot hand teleoperation," in *ABCM Symposium Series in Mechatronics*, vol. 5, 2012, pp. 1065–1074.

[17] A. Kheddar, "Teleoperation based on the hidden robot concept," *IEEE Transactions on Systems, Man, and Cybernetics-Part A: Systems and Humans*, vol. 31, no. 1, pp. 1–13, 2001.

[18] L.-C. Kuo, H.-Y. Chiu, C.-W. Chang, H.-Y. Hsu, and Y.-N. Sun, "Functional workspace for precision manipulation between thumb and fingers in normal hands," *Journal of electromyography and kinesiology*, vol. 19, no. 5, pp. 829–839, 2009.

[19] L. Biagiotti, F. Lotti, C. Melchiorri, and G. Vassura, "How far is the human hand? a review on anthropomorphic robotic end-effectors," 2004.

[20] T. Sugihara, "Solvability-unconcerned inverse kinematics based on levenberg-marquardt method with robust damping," in *2009 9th IEEE-RAS International Conference on Humanoid Robots*. IEEE, 2009, pp. 555–560.

[21] B. Gärtner and M. Hoffmann, "Computational geometry lecture notes1 hs 2012," *Dept. of Computer Science, ETH,Zürich, Switzerland*, 2013.

[22] C. Chen, Y. Hon, and R. Schaback, "Scientific computing with radial basis functions," *Department of Mathematics, University of Southern Mississippi, Hattiesburg, MS*, vol. 39406, 2005.

[23] M. Malvezzi, G. Gioioso, G. Salvietti, and D. Prattichizzo, "Syngrasp: A matlab toolbox for underactuated and compliant hands," *IEEE Robotics & Automation Magazine*, vol. 22, no. 4, pp. 52–68, 2015.

[24] C. Melchiorri, G. Palli, G. Berselli, and G. Vassura, "Development of the ub hand iv: Overview of design solutions and enabling technologies," *IEEE Robotics & Automation Magazine*, vol. 20, no. 3, pp. 72–81, 2013.